

# The JAERI superconducting linac based FEL

T. Shizuma, E.J. Minehara, N. Nishimori, R. Nagai, R. Hajima,  
M. Sawamura, N. Kikuzawa, T. Yamauchi, JAERI, Tokai, Japan

## Abstract

The JAERI superconducting rf linac has been developed to produce a high-power infrared free-electron laser (FEL). So far, a stable kW-level laser output has been achieved with improvements of the electron gun, the optical resonator as well as the beam transport optics. For increasing FEL power, energy-recovery experiments are planned in the next phase of the FEL development. The lattice design and simulated performance of the energy-recovery beam line are described.

## 1 INTRODUCTION

At the Japan Atomic Energy Research Institute (JAERI), a free electron laser (FEL) driven by superconducting linear accelerators has been constructed to produce a high power FEL at far-infrared (20-30 $\mu$ m) region. In 1998, a first lasing was achieved with an average output power of 0.1 kW in quasi-CW operation [1]. With improvements of the electron gun, the optical resonator, the electron beam transport optics [2, 3], in 2000, the average laser output power was reached to 1.7kW [4], which is the goal for the first phase project. In order to increase the FEL power, we plan to install an energy-recovery beam line as the second phase project. In this scheme, the electron beam is re-injected to the same rf modules as used for the acceleration, but at the decelerating phase. The beam power can then be transferred to the rf cavities, and recycled for acceleration. Therefore, an electron beam with a higher average current can be accelerated with minimum rf power supplement, which would enable to increase the average FEL power.

In this paper, we summarize the recent results of our high-power FEL operation in section 2. Design and simulated performance of the energy-recovery transport are presented in sections 3 and 4.

## 2 HIGH-POWER FEL OPERATION

The JAERI-FEL injector consists of a 230 kV electron gun and an 83.3 MHz sub harmonic buncher (SHB) followed by two units of a 500 MHz superconducting rf one-cell cryomodule. In order to prevent emittance growth due to space charge forces, a high voltage of 230 kV is applied. The electron gun parameters are listed in Table 1. The bunched beam is compressed by means of energy modulation of the SHB field. The path length between the SHB and the pre-accelerator is selected to optimize the longitudinal phase space parameters at the entrance to the first pre-accelerator.

The injected beam enters two units of a 7.5 MeV superconducting rf five-cells cryomodule. The accelerated

Table 1: Electron gun parameters

Accelerated voltage	230 kV
Cathode	Y646B
Charge per pulse	0.5~0.6 nC
RMS pulse width	0.34 ns
RMS beam radius	1.6 mm
Normalized RMS emittance	14 $\pi$ mm-mrad
Time jitters (rms)	23 ps

beam is then turned by 180° before reaching the undulator. The arc consists of three 60° bends with two sets of a quadrupole doublet. The beam is finally injected into the undulator placed at about 0.5 m downstream of the arc exit.

The major factors which enabled us the high power FEL operation recently achieved are followings;

- Shortening the electron bunch length and reducing the time jitters at the electron gun.
- Optimization of the drift length between the SHB and the pre-accelerator.
- Optimal beam transport optics.
- Increasing the output coupling efficiency by use of the insertable scraper.

The FEL parameters are summarized in Table 2.

Table 2: JAERI-FEL parameters

Kinetic energy	16.4 MeV
Average current	0.53 mA
Bunch length (rms)	2.5 ps
Peak current	100 A
Norm. emittance (rms) H/V	40/22 $\pi$ mm-mr
Wiggler period	3.3 cm
Number of period	52
$K_{rms}$	0.7
Optical cavity length	14.4 m
Rayleigh range	1.04 m
Mirror radii	6 cm
Mirror reflectivity	99 %
Repetition rate	10.4125 MHz
Macropulse duration (max.)	1 ms

## 3 DESIGN OF ENERGY-RECOVERY BEAM LINE

A schematic layout of the energy-recovery beam line is shown in Fig. 1. The first part of the injector for the energy-recovery transport is the same geometry for the

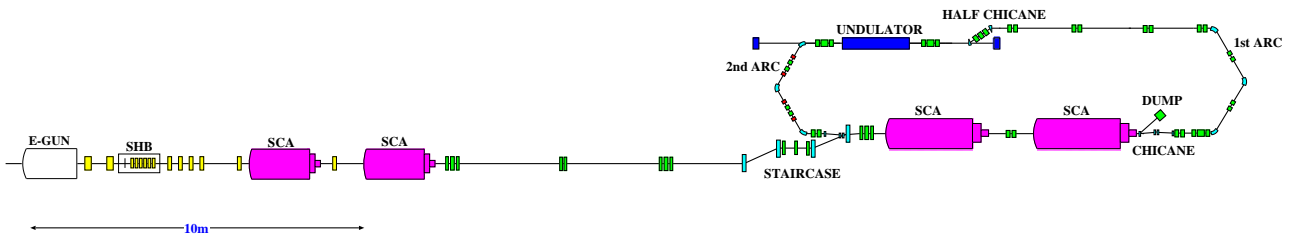


Figure 1: Schematic layout of the energy-recovery beam line.

non-energy-recovery operation described above. In order to merge the injected and recirculated beams, a magnetic buncher is necessary before the main cryomodule. For reducing the beam degradation, we chose a staircase buncher which satisfies achromatic condition and other factors required for the energy-recovery injector [5].

In the recirculating transport, the main-cryomodules and the  $180^\circ$  bend (1st arc) is the same as those described in section 2. Between them a four-dipole chicane is placed to transport the decelerated beam to the dump. After the undulator, the electron beam is turned by  $180^\circ$  for re-injection to the main-cryomodule. Although several arcs with both the achromaticity and isochronicity exist, we chose three  $60^\circ$  bends, similar to the first arc, with advantage in compactness, cost and compatibility. Since the electron beam has large energy spread ( $\sim 3\%$ ) after the FEL interaction, energy acceptance and second-order aberration are critical to decide the design of the second arc. To compensate the second-order aberrations such as  $T_{166}$ ,  $T_{266}$  and  $T_{566}$ , two families of sextupoles are added at both sides of the quadrupole doublet in the second arc [6].

## 4 SIMULATED PERFORMANCE

### 4.1 Injection beam line

The horizontal and vertical beam envelope functions are calculated with PARMELA [7] as shown in Fig. 2. Initial parameters used in the simulations are listed in Table 1. Since the space charge force causes a large emittance growth especially for low energy electrons, its effects to the transversal motion must be investigated. At the low energy (230 keV) region between the electron gun and the

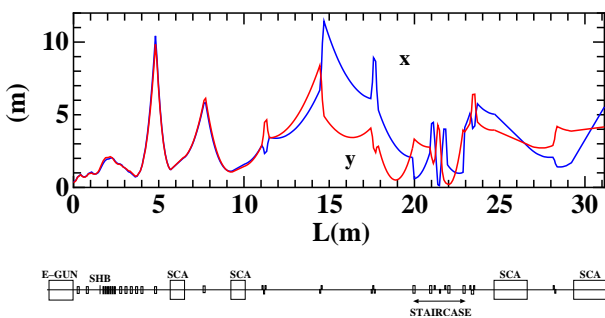


Figure 2: Horizontal and vertical beam envelope functions from the electric gun to the main-accelerator exit.

pre-accelerator, the emittance growth by the linear space charge [8] is most important, and this type of the emittance growth is known to be reduced by placing solenoid fields at the proper location [9]. The emittance compensation for the JAERI injector is done by parallel beam transport using a series of the solenoid lenses. The transversal emittance calculated with PARMELA increases to  $20\pi$  mm-mrad at the pre-accelerator entrance from  $14\pi$  mm-mrad at the gun exit.

For electrons at  $\sim 2$  MeV after the pre-accelerators, the emittance growth by the linear space charge becomes negligible. However, in the staircase buncher, an emittance growth from the space charge is again expected to be large. Both the electron beam energy and radial velocities are modified from magnet to magnet due to the space charge effect, causing a horizontal emittance growth [8]. The effect can be minimized when the beam enters with a waist to the buncher entrance in the bending plane. The normalized rms emittance is calculated with PARMELA including space charges as  $\epsilon_x = \epsilon_y = 20\pi$  mm-mrad at the entrance and  $\epsilon_x = 38\pi$ ,  $\epsilon_y = 25\pi$  mm-mrad at the exit.

The longitudinal motion with space charge included is also simulated using PARMELA. For optimal bunching, the applied voltage and the rf phase of the buncher is set as 75 kV and  $10^\circ$  off zero-crossing toward the decelerating direction. After the 4.5 m drifting space, the electron beam enters the first pre-accelerator. Since the velocity of the electrons is  $0.71c$  and the rf phase velocity of the cavity is speed-of-light, both the longitudinal and transversal rf focusing effects change with the rf phase of the first pre-accelerator. For optimizing the longitudinal phase and minimizing the transversal emittance, the rf phase of the first cavity is chosen as  $15^\circ$  off the maximum beam loading phase toward the debunching direction. Furthermore, the best longitudinal phase space distribution for the entrance to the staircase buncher with  $R_{56} = -0.34$  m is accomplished with  $35^\circ$  off-crest phase toward the bunching direction for the second pre-accelerator. Figure 3 shows the longitudinal phase space distributions at the entrance to the main cryomodule calculated with PARMELA. The axial beam parameters are obtained as rms bunch length  $\sigma_t = 9$  ps and rms energy spread  $\Delta E/E = 0.9\%$  at 2.6 MeV.

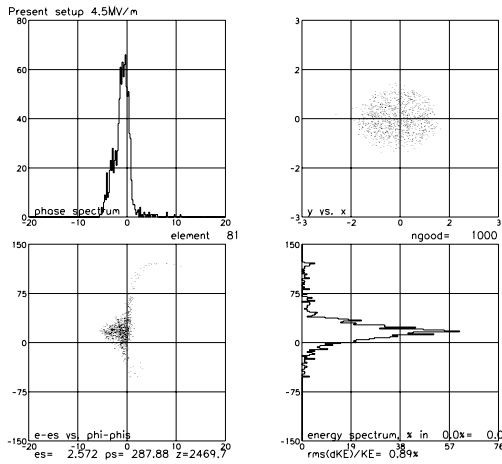


Figure 3: Various distributions of the longitudinal phase space at the entrance to the main cryomodule.

#### 4.2 Recirculating beam line

Figure 4 shows the horizontal and vertical betatron functions and the horizontal dispersion function calculated with DIMAD [10]. The betatron functions are less than about 12 m along the recirculating beam line. Since the bending angles of the dipoles in the  $180^\circ$  arc and the half chicane are large,  $60^\circ$  and  $45^\circ$ , the horizontal emittance would increase by coherent synchrotron radiation (CSR) force. To estimate its effects, we made a numerical calculation with elegant [11]. For a 9ps(rms) bunched beam with 0.6 nC, the emittance growth by CSR is estimated as  $\Delta\epsilon = 13$  at the first arc and  $6 \pi$  mm-mrad at the half chicane [12]. Assuming the growth is independent of the initial emittance, we estimate the horizontal emittance of  $41(=\sqrt{38^2 + 13^2 + 6^2}) \pi$  mm-mrad at the entrance to the undulator. In the second arc, the horizontal dispersion function is maximum ( $\eta_x = 0.6$  m) at the focusing quadrupoles. Therefore, the energy acceptance of the arc is determined by the quadrupole bore radius. Since the energy spread after the FEL interaction is estimated as about 3%, the bore radius of 35 mm is enough to accept the entire beam.

### 5 SUMMARY

At the JAERI FEL facility, the lasing output power of 1.7 kW was recently demonstrated. The main factors of the high power operation were improvements of the electron gun, the optical resonator, the beam transport optics. The energy-recovery beam line for the second phase project has been designed to increase the FEL power. A staircase magnetic array was chosen for the injection buncher to merge the injected and recirculated beams. For the recirculating transport, a  $180^\circ$  arc consisting of three  $60^\circ$  bends together with quadrupole doublets and sextupoles will be added to the existing beam line. Both the transversal and longitudinal electron motions were investigated by PARMELA and DIMAD.

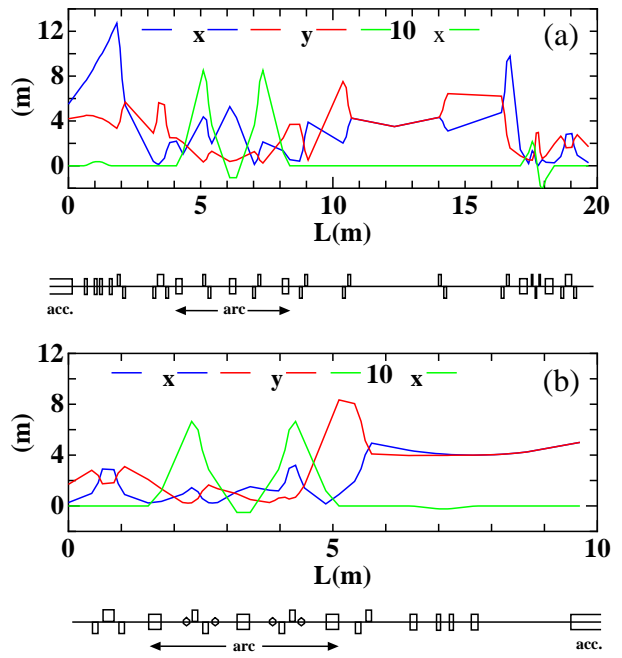


Figure 4: Horizontal and vertical beam envelope functions from the main-accelerator exit to the undulator entrance (a), and from the undulator exit to the re-injection point at the main-accelerator (b).

### 6 REFERENCES

- [1] E.J. Minehara et al., Nucl.Inst.Meth. A429 (1999) 9.
- [2] N. Nishimori et al., Nucl.Inst.Meth. A445 (2000) 432.
- [3] R. Nagai et al., Proceedings in the 22nd Int.FEL conf., Durham 2000.
- [4] N. Nishimori et al., Proceedings in the 22nd Int.FEL conf., Durham 2000.
- [5] T. Shizuma et al., Proceedings in the 7th EPAC, Vienna 2000.
- [6] R. Hajima et al., Nucl.Inst.Meth. A445 (2000) 384.
- [7] L.M. Young, LA-UR-96-1835.
- [8] B.E. Carlsten and T.O. Raubenheimer, Phys.Rev.E 51(1995)1453.
- [9] B.E. Carlsten, Nucl.Inst.Meth. A285 (1989) 313.
- [10] R.V. Servranckx, TRI-DN-93-K233, 1993.
- [11] <http://www.aps.anl.gov/asd/oag/oagPackages.shtml>
- [12] R. Hajima et al., Proceedings in the 7th EPAC, Vienna 2000.